Proceedings of the 12th International Conference on the Stability of Ships and Ocean Vehicles, 14-19 June 2015, Glasgow, UK.

Influence of Rudder Emersion on Ship Broaching Prediction

Liwei Yu, *School of Naval Architecture and Ocean Engineering, Shanghai Jiao Tong University (SJTU)*, liwyu55@sjtu.edu.cn

Ning Ma*, *State Key Laboratory of Ocean Engineering, SJTU*, ningma@sjtu.edu.cn.cn

Xiechong Gu, *State Key Laboratory of Ocean Engineering, SJTU*, xcgu@sjtu.edu.cn

ABSTRACT

Broaching is recognized as one of the major causes of ship capsizing in adverse quartering seas. Loss of rudder effectiveness due to rudder emersion is believed to be very important for broaching. Therefore in the paper, a 6-DOF unified model considering sea-keeping motion at low frequency, manoeuvring motion and rudder propeller hydrodynamics is developed for the numerical analysis of broaching of the ITTC ship A2. A modified model of rudder is proposed to account for the effect of wave orbital velocity and the variation of rudder area and aspect ratio. The modified model of rudder is compared with the original model. Then numerical simulations are conducted in different ship speeds and wave heights, and the influence of rudder emersion on broaching motion is investigated. Results show that rudder immersed depth decreases dramatically and rudder inflow velocity is reduced by wave orbital velocity when surf-riding happens. It is also concluded that rudder emersion is the key factor for the emergence of broaching motion. Moreover the influence of rudder emersion seems to take effect only when Froude number is high.

Keywords: *Broaching, Surf-riding, Unified model, Rudder emersion*

1. INTRODUCTION

Ships have much higher possibility of capsizing when sailing in adverse following and quartering seas comparing to head sea condition. Broaching is one of the major causes of capsizing in following and quartering seas. When sailing in astern seas, ship may encounter large wave induced yaw moment and rudder may lose its course-keeping capability. These will cause ship heading to change suddenly and broaching occurs. Broaching often occurs on small ship and naval vessel with high speed. According to IMO Sub-Committee on Ship Design and Construction (SDC), ship is considered to be vulnerable to broaching if Fn>0.3 or L_{BP}<200m (IMO SDC, 2014).

Since the pioneering work of Grim (1951) based on analytical formula, researches on surf-riding and broaching are conducted through theoretical analyses (Umeda, 1999; Makov, 1969; Spyrou, 1996), numerical simulations (Umeda & Hamamoto, 2000; Umeda & Hashimoto, 2002; Yu, Ma, & Gu, 2014) and model experiments (Umeda et al., 1999). As an output of these continuous efforts, the amendments to Part B of the 2008 IS code to assess broaching are proposed recently in IMO (IMO SDC, 2014). However as a strongly nonlinear phenomenon, broaching is influenced by various factors and detailed investigation needs to be conducted.

Loss of rudder effectiveness due to rudder and propeller emersion is believed to be an important factor for the occurrence of broaching. Rudder and propeller emersion is observed in free running model experiment when broaching happens (Araki et al., 2012). Renilson (1982) conducted numerical and experimental study on broaching for ship with standard rudder and rudder with 1/2 depth. Rudder force derivatives in wave were considered in a simplified way. Results showed that loss in rudder effectiveness caused by emersion had an important influence on broaching. Furthermore, Umeda & Kohyama (1990) pointed out that propeller thrust coefficient dropped dramatically when surf-riding happened due to high advance coefficients in wave. This could reduce rudder inflow velocity induced by propeller, in turn weakening rudder force. They also mentioned the possible influence of wave orbital velocity and rudder emersion on surf-riding and broaching. Tigkas & Spyrou (2012) conducted steady-state analysis and bifurcation analysis with a 6 DOF model. In the model, loss of rudder effectiveness was considered by changing rudder area and aspect ratio according to its instantaneous draught. However the influence of rudder on broaching was not further discussed in the paper. Araki et al. (2012) proposed a 6-DOF model with a full consideration of rudder and propeller emersion for the broaching prediction of a tumblehome vessel. In the model the unexpected yaw moment caused by the emersion of twin propellers was also taken into account. Through comparison with experiment and 4-DOF numerical simulation results, it showed that rudder and propeller emersions could be a crucial factor for broaching.

However improvements on the modeling of rudder and propeller are still needed for a better understanding of rudder's influence on broaching. Critical factors such as wave orbital velocity, rudder inflow velocity, propeller and rudder wake near free surface and vortex shedding at rudder edge should be considered in the numerical model. Although very few data is available for loss of rudder effectiveness caused by rudder and propeller emersion, one can be inspired from researches on reduction of rudder performance in ship ballast condition. Experiments show that rudder force coefficients are reduced due to air bubble and wave making on free surface when rudder is out of water (Lu et al., 1981). Flow straightening coefficient and rudder wake differ significantly with different trims (Liu, Huang, & Deng, 2010) while the hull-rudder interaction coefficients differ slightly for different drafts and trims (Nagarajan et al., 2008).

Therefore in order to investigate rudder's influence on broaching, the 6-DOF weakly nonlinear model proposed by Yu, Ma, & Gu (2012) is adopted for the simulation of broaching motion of the ITTC ship A2 in following and quartering seas. The model couples the manoeuvring and seakeeping motion based on the unified theory. Additionally, modelling of rudder and propeller is modified to account for the effect of wave orbital velocity, change of rudder area and aspect ratio and reduction of rudder inflow velocity. Through the analysis of the numerical results, the reduction of rudder steering capability in adverse following and quartering seas and its influence on broaching motion is investigated.

2. MATHEMATICAL MODEL

In the present numerical model, a combined seakeeping and manoeuvring analysis is carried out based on the unified theory. The modelling of rudder is modified to take the effect of rudder emersion into account.

2.1 6-DOF Weakly Nonlinear Model

In the unified model, the manoeuvring motion is simulated using a 3-DOF surge-sway-yaw MMG model:

$$\begin{bmatrix} m-\bar{X}_{\dot{U}} & 0 & 0 \\ 0 & -m+\bar{Y}_{\dot{V}} & -mx_G+\bar{Y}_{\dot{R}} \\ 0 & -mx_G+\bar{N}_{\dot{V}} & -I_z+\bar{N}_{\dot{R}} \end{bmatrix} \begin{bmatrix} \dot{u} \\ \dot{v} \\ \dot{R} \end{bmatrix} + \begin{bmatrix} 0 & -mR & 0 \\ 0 & \bar{Y}_V & -mU+\bar{Y}_R \\ 0 & \bar{N}_V & -mx_GU+\bar{N}_R \end{bmatrix} \begin{bmatrix} u \\ v \\ R \end{bmatrix} = \begin{bmatrix} \bar{X}_{HO} \\ \bar{Y}_{HO} \\ \bar{N}_{HO} \end{bmatrix} + \begin{bmatrix} \bar{X}_\delta \\ \bar{Y}_\delta \\ \bar{N}_\delta \end{bmatrix} + \begin{bmatrix} -R(U) \\ +(1-t)T(U) \\ 0 \\ 0 \end{bmatrix} \quad (1)$$

where m and I represent the ship mass and moment of inertia. u, v, R denote surge, sway and yaw velocity. (X_δ, Y_δ, N_δ), $R(U)$ and $T(U)$ are defined as rudder force, ship resistance and propeller thrust respectively. t is the propeller thrust deduction factor. (X_{HO}, Y_{HO}, N_{HO}) is higher order hull hydrodynamic force:

$$\begin{aligned} \bar{X}_{HO} &= X_{vv}v^2 + X_{vr}vr + X_{rr}r^2 \\ \bar{Y}_{HO} &= Y_{vvr}v^2r + Y_{vrr}vr^2 + Y_{vvv}v^3 + Y_{rrr}r^3 \\ \bar{N}_{HO} &= N_{vvr}v^2r + N_{vrr}vr^2 + N_{vvv}v^3 + N_{rrr}r^3 \end{aligned} \quad (2)$$

The sea-keeping motion is simulated by a 6-DOF model based on the IRF approach. The equation of motion can be written as:

$$\begin{aligned} &\sum_{j=1}^{6}\left[\left(m_{ij}+a_{ij}(\infty)\right)\dot{v}_j(t) + \int_0^t R_{ij}(t-\tau)v_j(\tau)d\tau + F_i^{res}(t)\right] \\ &= F_i^{FK}(t) + F_i^{dif}(t) + (\bar{K}_\delta, when\ i=4) \quad (i=1,...,6) \end{aligned} \quad (3)$$

where m_{ij} and $a_{ij}(\infty)$ stand for the ship mass and the infinite-frequency added mass. The nonlinear restoring forces, F-K forces and diffraction forces are denoted as $F_i^{res}(t), F_i^{FK}(t), F_i^{dif}(t)$ respectively.

According to the IRF approach, the radiation and diffraction forces are calculated in frequency domain by the strip theory and transferred into time domain using the retardation function $R_{ij}(\tau)$. The nonlinear restoring and Froude-Kriloff forces are calculated through pressure integration on instantaneous wetted surfaces. The hull and upper deck consist of several NURBS surfaces are demonstrated in Figure 1.

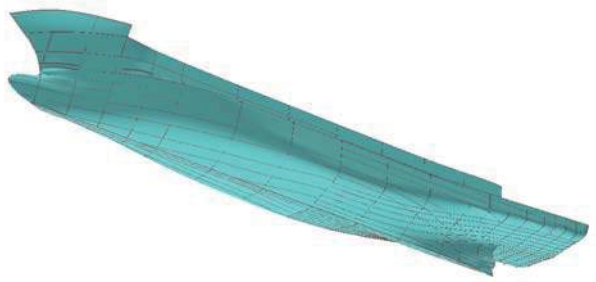

Figure 1 Hull NURBS surface of ITTC ship A2

In the unified model, the manoeuvring and seakeeping models described above are solved in different time scale. The total ship motion is calculated by combining the two motions referring to different coordinate system together:

$$\begin{aligned} &\left[X_T, Y_T, Z_T, \Phi_T, \Theta_T, \Psi_T\right] = \left[x^0, y^0, z^0, \phi^0, \theta^0, \psi^0\right] \\ &+\left[\int_0^t U_T dt, \int_0^t V_T dt, \int_0^t W_T dt, \int_0^t P_T dt, \int_0^t Q_T dt, \int_0^t R_T dt\right] \end{aligned} \quad (4)$$

where the subscript T indicates the total motion, and superscript 0 means the initial value for the time t=0.

2.2 Modelling of Rudder and Propeller

The rudder forces and propeller thrust are calculated as follows:

$$\begin{cases} \bar{X}_\delta = -0.5(1-t_R)\rho A_R {U_R}^2 C_N \sin\alpha_R \sin\delta \\ \bar{Y}_\delta = -0.5(1+a_H)\rho A_R {U_R}^2 C_N \sin\alpha_R \cos\delta \\ \bar{N}_\delta = -0.5(GR_L + a_H x_H)\rho A_R {U_R}^2 C_N \sin\alpha_R \cos\delta \\ \bar{K}_\delta = -GR\bar{Y}_\delta \end{cases} \quad (5)$$
$$T(U) = \rho K_T D_P^4 n^2$$

where K_δ denotes rudder roll moment. A_R, U_R, GR, GR_L indicate the rudder area, the inflow velocity, the vertical and longitudinal distance between center of gravity and point of rudder force. n, D_p, K_T represent the propeller rotation rate, diameter and thrust coefficient.

In order to account for the effect of rudder emersion, the model for rudder forces and moments need to be modified. Firstly rudder

inflow velocity and propeller advance coefficient are modified to incorporate wave orbital velocity:

$$U_R = \sqrt{(u_r + \bar{u}_w)^2 + v_r^2}$$
$$J_w = \frac{(1-\omega_p)U\cos\beta + \bar{u}_w}{nD_P} \quad (6)$$
$$K_{Tw} = a_0 + a_1 J_w + a_2 J_w^2$$

where u_r, v_r denote the longitudinal and transversal rudder inflow velocity. ω_p, β denote the propeller wake fraction, and ship drift angle. $\bar{u}_w$ is the longitudinal component of mean value wave orbital velocity around rudder as shown in Figure 2:

$$u_w = C_w k A_w e^{kz}\cos(kx - \omega t) \quad (7)$$

where C_w, A_w, k, ω stand for the wave celerity, wave amplitude, wave number and frequency.

Furthermore, the variation of rudder area A_{Rw}, and aspect ratio λ_w due to rudder emersion are obtained from instantaneous wetted surfaces. The rudder force coefficient C_N is still determined by Fujii's prediction formula (Ogawa & Kasai, 1978):

$$\lambda_w = h_w / b$$
$$C_N = 6.13\lambda_w / (2.25 + \lambda_w) \quad (8)$$

where b denotes rudder width. h_w is rudder immersed depth which is calculated from the distance between free surface and rudder bottom considering 6-DOF ship motion as shown in Figure 2.

Due to the limitation of present model, the variation of other factors including hull-rudder interaction coefficients, flow straightening coefficient and rudder wake are not yet taken into account.

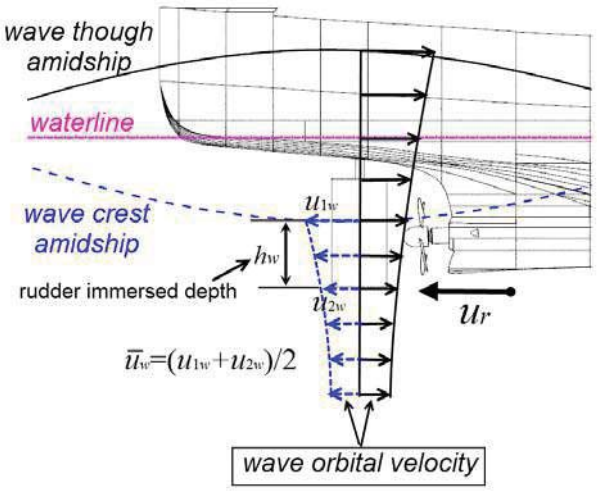

Figure 2 Wave oribital velocity around rudder

3. MODEL VERIFICATION

3.1 Ship Model

The subject ship used for the verification of the weakly nonlinear numerical model accounting for rudder emersion is the ITTC ship A2 fishing vessel(NAOE Osaka University, 2015). Main particulars of the ship and its model are shown in Table 1.

The autopilot system are modeled as follows:

$$T_E\dot{\delta} + \delta = -K_p(\chi - \chi_c) \quad (9)$$

Where the time constant T_E is 0.63s, δ is the rudder angle, $\dot{\delta}$ is rudder rate, χ is the yaw angle, and χ_c is the desired course.

All other data needed for the numerical simulation including hull geometry, hydrodynamic derivatives, rudder and propeller characteristics, roll viscous damping can be found in NAOE Osaka University (2015).

Table 1 Main particulars of ITTC ship A2

Ship		1/15 model
Length between per-pendiculars, L_{pp}(m)	34.5	2.3
Breadth, B(m)	7.60	0.507
Depth, D(m)	3.07	0.205
Fore draught, d_f(m)	2.5	0.166
Aft draught, d_a(m)	2.8	0.176
Mean draught, d(m)	2.65	0.186
Block coefficient, C_B	0.597	0.597
Radius of gyration, roll, k_{xx}/L_{pp}	0.108	0.108
Radius of gyration, pitch yaw, k_{yy}/L_{pp}, k_{zz}/L_{pp}	0.302	0.302
Longitudinal position of Buoyancy, L_{CB}(m)	1.31m aft	0.087m aft
Longitudinal position of Floatation, L_{CF}(m)	3.94m aft	0.263m aft
Metacentric height, GM(m)	1.00	0.0667
Natural roll period,T_R(s)	7.4	1.9
Rudder		
Area, A_R(m^2)	3.49	0.0155
Rudder aspect ratio, Λ	1.84	1.84
Rudder height, h(m)	2.57	0.171

3.2 Validation of rudder modelling

The 6-DOF weakly nonlinear model for the simulation of surf-riding and broaching in astern seas are validated qualitatively based on experiment results of ITTC ship A2 in Yu, Ma, & Gu, (2014). In this paper, the model is further modified based on the method in section 2.2 to account for the effect of rudder emersion. However there is no experimental data for rudder emersion such as rudder immersed depth, wave orbital velocity around rudder and rudder forces and moments. Thus in this paper, the modified model accounting for rudder emersion is only validated through comparison with the original model without rudder emersion. The results of comparison are demonstrated in Figure 3

In Figure 3, (a), (b), (c) and (d) are time history of ship yaw, roll, pitch and heave motion. (e) and (f) are the time history of wave orbital velocity u_w and rudder immersed depth h_w. The dashed line is results for the original model without rudder emersion, while the solid line is results for the modified model with rudder emersion.

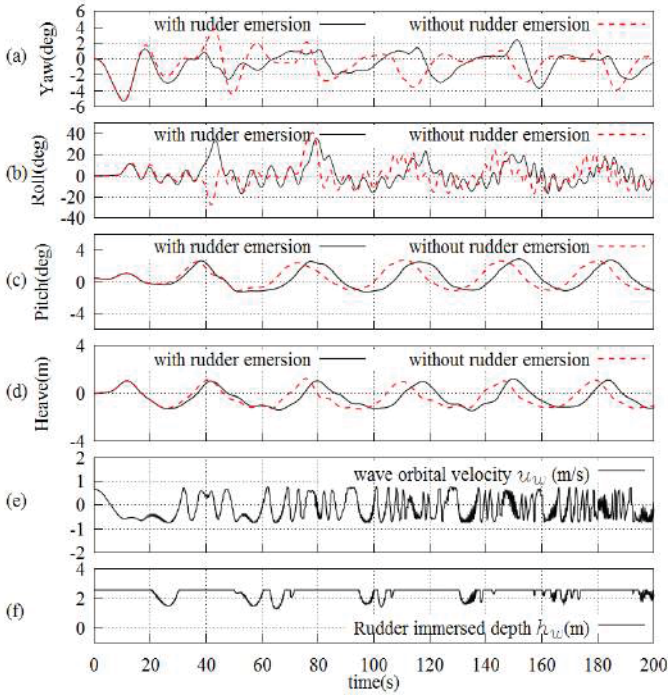

Figure 3 Comparison of ship motions between with and without rudder emersion (H_w=4m, λ/L_{pp}=1.637, Fn=0.40 and χ=-10 deg)

From Figure 3, it can be identified that ship is doing periodic motion in astern sea with and without rudder emersion. However the differences on ship motion between with and without rudder emersion can be easily found. This can be explained by the rudder emersion in astern sea. As shown in Figure 3(a)(b)(c), yaw, roll and pitch motion of the two model are almost the same before 20s. While the time is around 20-30s, rudder emersion starts, rudder immersed depth decreases and rudder inflow velocity is reduced by wave orbital velocity as shown in Figure 3(e)(f). At the same time, there is an overshot on yaw angle for the modified model (solid line) compared to the original model (dashed line) as shown in Figure 3(a). This overshoot proves that rudder emersion can cause loss of rudder effectiveness and steering capability in astern sea.

Therefore through comparison between results of the original model without rudder emersion and the modified model with rudder emersion, the modified model is verified to be able to account for the effect of rudder emersion. Its influence on broaching motion will be investigated in the next chapter.

4. SIMULATION RESULTS

4.1 Calculation Cases

Numerical simulations using the modified 6-DOF weakly nonlinear model accounting for rudder emersion are conducted to investigate the influence of rudder behaviour on broaching motion. The subject ship is ITTC ship A2, and calculation cases including 5 ship speeds and 11 wave heights are shown in Table 2.

Table 2 Cases for numerical simulation

No.	Fn	V(m/s)	H_w(m)	λ/L_{pp}	χ	C_{wx}(m/s)	ω_e
1-#	0.3	5.52	3.6~6	1.637	-30	8.13	0.563
2-#	0.33	6.07	3.6~6	1.637	-30	8.13	0.516
3-#	0.36	6.62	3.6~6	1.637	-10	9.25	0.453
4-#	0.40	7.36	3.6~6	1.637	-10	9.25	0.295
5-#	0.43	7.91	3.6~6	1.637	-10	9.25	0.228

Where "#" denotes numbers for different wave height H_w. Fn stands for Froude number. H_w, λ, χ are wave height, length and angle, ω_e is encounter frequency taking into account the nonlinearity caused by high wave amplitudes (see Eqn.(10), Umeda et al., 1999). V, C_{wx} denotes ship nominal speed and wave celerity in x direction. They satisfy the followings:

$$\begin{aligned} &\omega^2 = gk(1+k^2 H_w^{\ 2}/4) \\ &\lambda = 2\pi/k, \omega_e = \omega - kU\cos(\chi), U = \mathrm{Fn}\sqrt{gL_{pp}}, \\ &C_w = \lambda\sqrt{gk}/2\pi,\ C_{wx} = C_w\cos(\chi) \end{aligned} \tag{10}$$

In order to evaluate the influence of rudder emersion, simulations using the original model without rudder emersion with the same cases are also conducted for comparison.

4.2 Result Analysis

The simulation results obtained from the modified model and the original model are demonstrated in Figure 4, 5 and 6. In Figure 4 and 5, results of the case No. 4-5 and 5-4 are shown. The left figure shows the result of the original model, while the right one shows result of the modified model. (a)-(g) represents the time history of yaw & rudder angle, roll angle, pitch & heave, ship velocity, ship relative position in wave, wave orbital velocity around rudder u_w and rudder immersed depth h_w. Ship relative position in wave is the distance of ship centre of buoyancy to wave though multiplied with wave number k leading to a value within $[0, 2\pi]$.

From Figure 4, it can be found that ship relative position in wave keeps almost constant within the time range 45-85s for the original and modified model. Meanwhile, the pitch angle stays almost unchanged and the ship is accelerated to wave celerity as shown in Figure 4(c) and (d). This indicates that surf-riding occurs for both models. Because ship relative position in wave is constant when surf-riding happens, wave orbital velocity also keeps constant as presented in Figure 4 right (f). Moreover as shown in Figure 4 right (f)(g), for the modified model rudder immersed depth decreases dramatically even to zero and rudder inflow velocity is reduced by wave orbital velocity when surf-riding happens. Thus the rudder effectiveness is significantly reduced and loss its course keeping capability, which are confirmed by the sudden increase of ship yaw angle despite hard turning of rudder to the opposite side as shown in Figure 4 right (a) within the time range 45-85s. Broaching almost happens. However after 85s, ship escapes from surf-riding, rudder retain its steering capability and ship turns back to original course. That is to say, ship motion by the modified model is further categorized as surf-riding and nearly broaching due to the influence of rudder emersion, while ship motion by the original model can only be categorized as surf-riding.

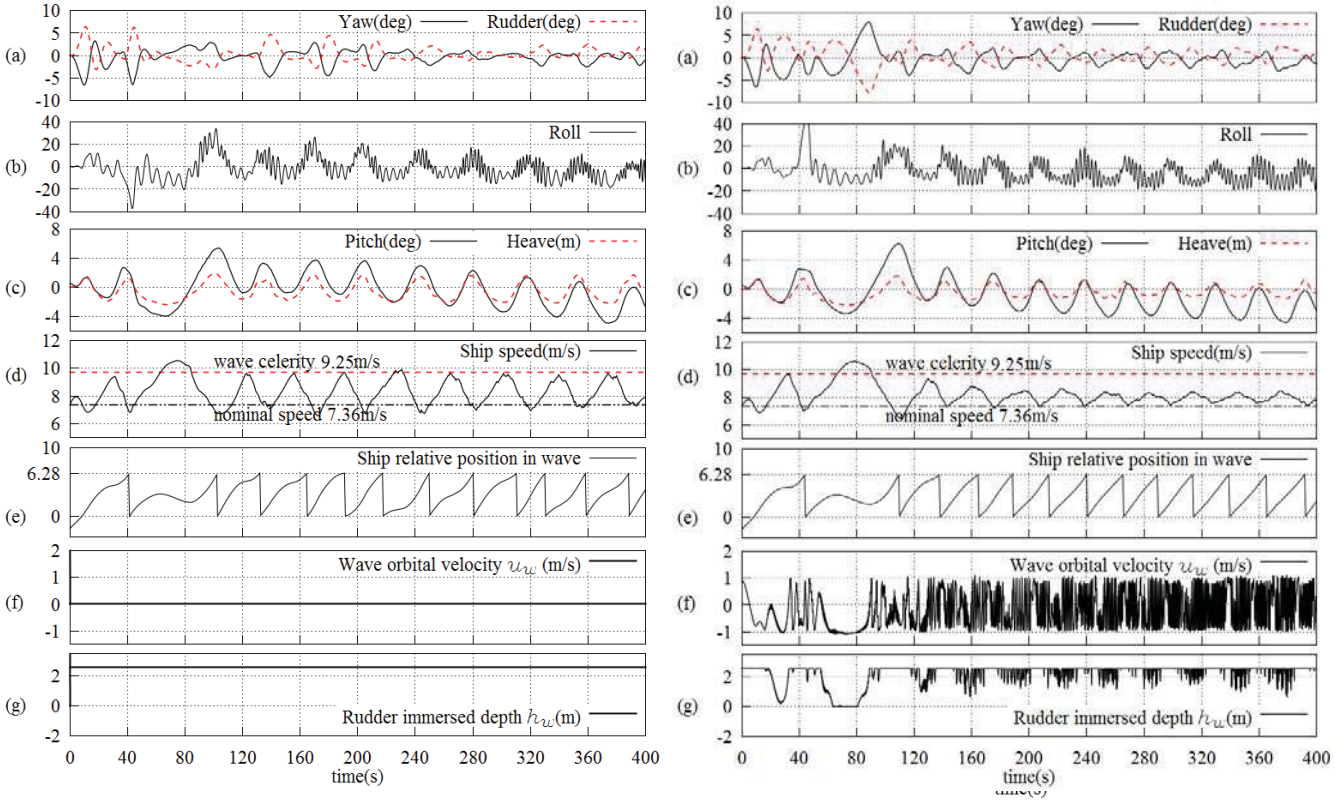

Figure 4 Simulation results of case 4-5 (H_w=4.6m, λ/L_{pp}=1.637, Fn=0.40 and χ=-10 deg)
Left: the original model; Right: the modified model

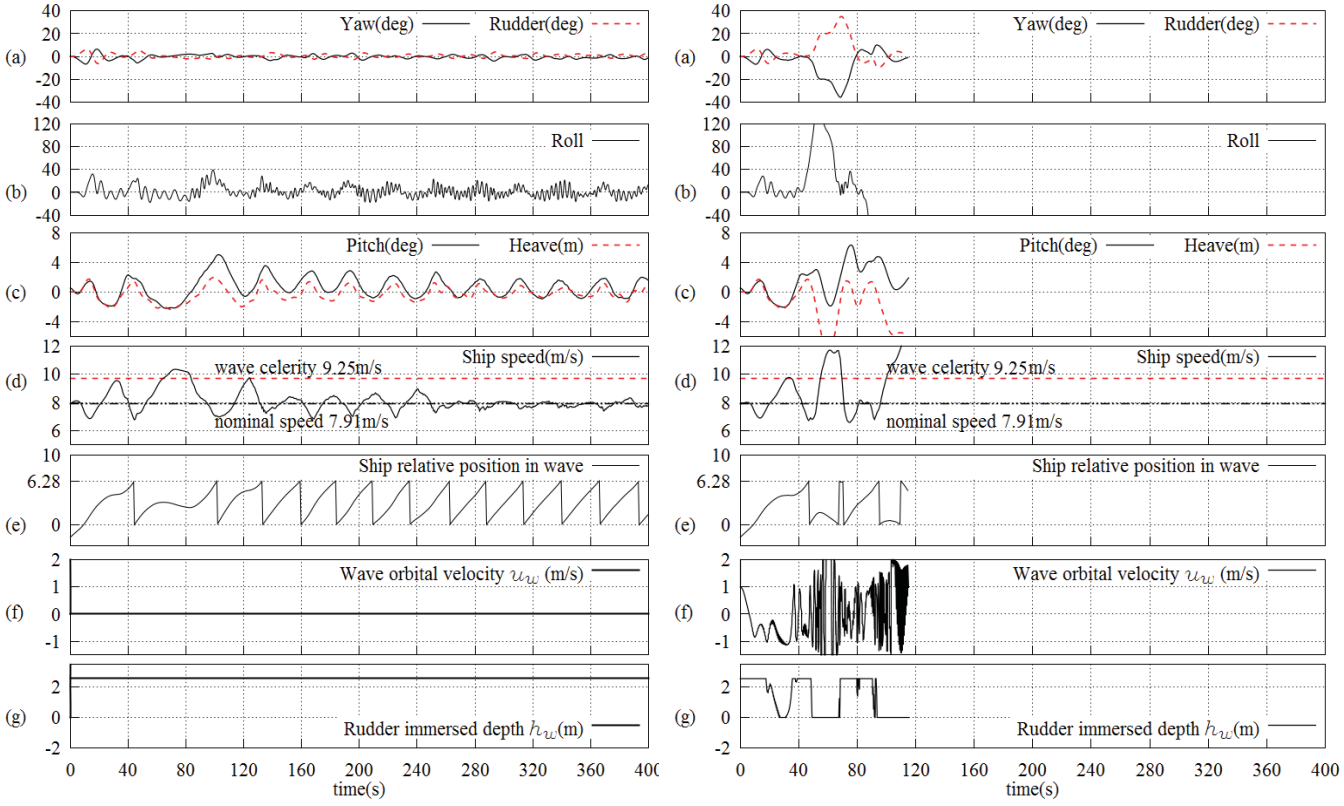

Figure 5 Simulation results of case 5-4 (H_w=4.8m, λ/L_{pp}=1.637, Fn=0.43 and χ=-10 deg)
Left: the original model; Right: the modified model

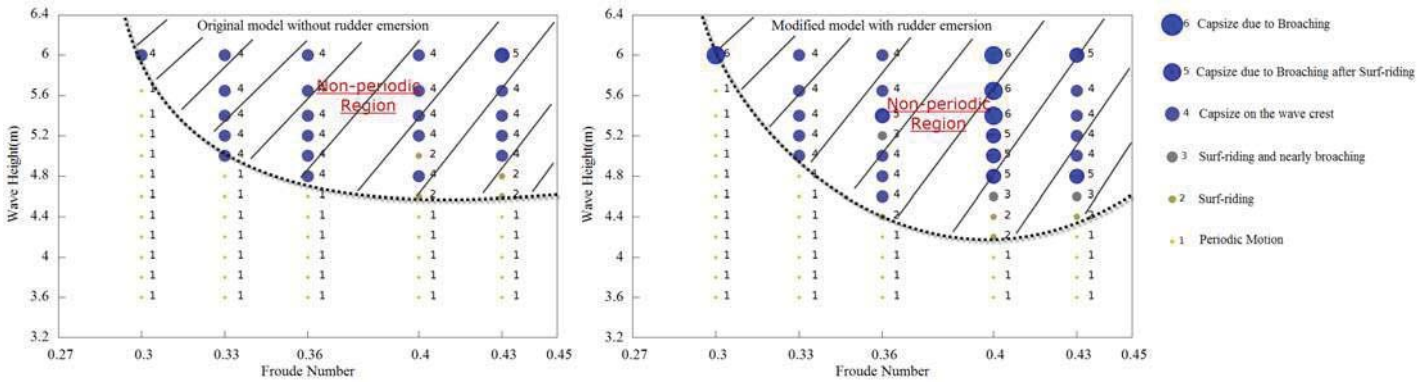

Figure 6 Comparison on simulation results of different cases (Left: the original model; Right: the modified model. The heading angle of cases with Fn=0.30 and 0.33 is -30 deg, while the heading angle of cases with Fn=0.36, 0.40 and 0.43 is -10 deg which are chosen based on the model experiments of Umeda et al., 1999)

Furthermore in Figure 5, the difference between the original and modified model becomes more obvious. The ship motion by the original model is categorized as surf-riding. Meanwhile, the motion by the modified model is categorized as capsize due to broaching after surf-riding. As shown in Figure 5 right, ship velocity is accelerated to wave celerity after 50s and rudder lose its steering capability due to emersion. Yaw angle increases suddenly despite max rudder control is applied. Roll angle also starts to raise and eventually causes ship to capsize. Thus capsize due to broaching after surf-riding has been demonstrated by the modified model. However in Figure 5 left, only surf-riding occurs due to the underestimate on the influence of rudder emersion in the original model.

According to the results presented in Figure 4 and 5, rudder emersion occurs and rudder immersed depth and inflow velocity decrease when surf-riding happens. If these effects are considered in the numerical model, loss of rudder effectiveness can cause sudden increase of yaw angle and even broaching. Therefore rudder emersion is the key factor for the emergence of broaching motion. This conclusion is confirmed by the results shown in Figure 6.

In Figure 6, the results of all the calculation cases including 5 ship speeds and 11 wave heights are presented. The ship motions response are categorized into 6 types: 1 Periodic Motion, 2 Surf-riding, 3 Surf-riding and nearly broaching, 4 Capsize on the wave crest, 5 Capsize due to Broaching after Surf-riding and 6 Capsize due to Broaching. From Figure 6, it is found that for the modified model with rudder emersion, non-periodic motion especially broaching is more likely to be aroused than for the original model. Additionally it is found that the difference between the two models exists mainly in Fn≥0.36. That is to say, the influence of rudder emersion mainly takes effect in Fn≥0.36.

5. CONCLUSIONS

In this paper, the 6-DOF weakly nonlinear model proposed by Yu, Ma, & Gu (2012) is adopted for the simulation of broaching motion of the ITTC ship A2 in following and quartering seas. Modelling of rudder and propeller is modified to account for change of rudder area and aspect ratio and reduction of rudder inflow velocity due to wave orbital velocity. Then numerical simulations are conducted in different ship speeds and wave heights. Through analysis of the results, the influence of rudder emersion on broaching

motion is investigated. The following conclusions are drawn:

1. During periodic motion, wave orbital velocity is oscillating, which has no effect on rudder inflow velocity. However when surf-riding happens, wave orbital velocity on rudder keeps almost constant, and the reduction on rudder inflow velocity cannot be neglected.

2. When surf-riding happens, rudder immersed depth decreases dramatically and rudder emersion effect is significant.

3. The loss of rudder effectiveness caused by rudder emersion and wave orbital velocity is the key factor for the emergence of broaching motion in quartering seas.

4. The influence of rudder emersion seems to take effect when Froude number is high and surf-riding is expect to occur.

However modelling of rudder still needs to be verified through experiments. Factors like variation of hull-rudder interaction coefficients, flow straightening coefficient and the thrust reduction due to propeller emersion should also be considered in the model.

6. REFERENCE

Araki, M., Umeda, N., Hashimoto, H., & Matsuda, A. (2012). An Improvement of Broaching Prediction with a Nonlinear 6 Degrees of Freedom Model. Journal of the Japan Society of Naval Architects and Ocean Engineers, 14, 85–96.

Grim, O. (1951). Das Schiff in von achtern auflaufender. Schiffbau-Versuchsanstalt.

IMO SDC1/INF.8 ANNEX 15. (2014). Proposed Amendments to Part B of the 2008 IS CODE to Assess the Vulnerability of Ships to the Broaching Stability Failure Mode. London, UK.

Liu, X., Huang, G., & Deng, D. (2010). Research of interaction force coefficients based on model test in loading condition. Journal of Shanghai Jiaotong University (Science), *15*(2), 168–171. doi:10.1007/s12204-010-8033-x

Lu, N., Zhu, H., Fei, W., & Wang, W. (1981). Experimental Study on Open Rudders. Journal of Shanghai Jiaotong University, *2*, 1.

Makov, Y. (1969). Some results of theoretical analysis of surf-riding in following seas. T Krylov Soc, (126), 4.

Nagarajan, V., Kang, D. H., Hasegawa, K., & Nabeshima, K. (2008). Comparison of the mariner Schilling rudder and the mariner rudder for VLCCs in strong winds. Journal of Marine Science and Technology, 13(1), 24–39.

NAOE Osaka University. (2015). Sample ship data sheet: ITTC A2 fishing vessel. Retrieved from http://www.naoe.eng.osaka-u.ac.jp/imo/a2

Ogawa, A., & Kasai, H. (1978). On the mathematical model of manoeuvring motion of ships. International Shipbuilding Progress, 25(292).

Renilson, M. R. (1982). An investigation into the factors affecting the likelihood of broaching-to in following seas. In Proceedings of the 2nd International Conference on Stability of Ships and Ocean Vehicles.

Spyrou, K. J. (1996). Dynamic instability in quartering seas : The behavior of a ship during broaching. Journal of Ship Research, 40(1).

Tigkas, I., & Spyrou, K. J. (2012). Continuation Analysis of Surf-riding and Periodic Responses of a Ship in Steep Quartering Seas. In Proceedings of the 11th International Conference on the Stability of Ships and Ocean Vehicles (pp. 337–349).

Umeda, N. (1999). Nonlinear dynamics of ship capsizing due to broaching in following and quartering seas. Journal of Marine Science and Technology, 4(1), 16–26. doi:10.1007/s007730050003

Umeda, N., & Hamamoto, M. (2000). Capsize of ship models in following/quartering waves: physical experiments and nonlinear dynamics. *Philosophical* Transactions of the Royal Society of London. Series A: Mathematical, Physical and Engineering Sciences, 358(1771), 1883–1904. doi:10.1098/rsta.2000.0619

Umeda, N., & Hashimoto, H. (2002). Qualitative aspects of nonlinear ship motions in following and quartering seas with high forward velocity. Journal of Marine Science and Technology, 6(3), 111–121. doi:10.1007/s007730200000

Umeda, N., & Kohyama, T. (1990). Surf-riding of a ship in regular seas. Journal of Kansai Society of Naval Architects, 11.

Umeda, N., Matsuda, A., Hamamoto, M., & Suzuki, S. (1999). Stability assessment for intact ships in the light of model experiments. Journal of Marine Science and Technology, *4*(2), 45–57. doi:10.1007/s007730050006

Yu, L., Ma, N., & Gu, X. (2012). Study on Parametric Roll and Its Rudder Stabilization Based on Unified Seakeeping and Maneuvering Model. In 11th Internationalconference on the Stability of Ships and Ocean Vehicles. Greece.

Yu, L., Ma, N., & Gu, X. (2014). Numerical Investigation into Ship Stability Failure Events in Quartering Seas Based on Time Domain Weakly Nonlinear Unified Model. In Proceedings of the 14th International Ship Stability Workshop (pp. 229–235). Kuala Lumpur, Malaysia.